23rd Australasian Conference on the Mechanics of Structures and Materials

2014

Dynamic foundation-structure interaction modelling using the coupled IGA-SBIGA method

M Li
Griffith University

Y Zhang
Chinese Academy of Sciences

Publication details

Li, M, Zhang, Y 2014, 'Dynamic foundation-structure interaction modelling using the coupled IGA-SBIGA method', in ST Smith (ed.), *23rd Australasian Conference on the Mechanics of Structures and Materials (ACMSM23)*, vol. II, Byron Bay, NSW, 9-12 December, Southern Cross University, Lismore, NSW, pp. 861-866. ISBN: 9780994152008.

23rd Australasian Conference on the Mechanics of Structures and Materials (ACMSM23)
Byron Bay, Australia, 9-12 December 2014, S.T. Smith (Ed.)

DYNAMIC FOUNDATION-STRUCTURE INTERACTION MODELLING USING THE COUPLED IGA-SBIGA METHOD

M. Li*
Smart Water Research Centre, Griffith University, Gold Coast Campus
Gold Coast, QLD, 4222, Australia. m.li@griffith.edu.au (Corresponding Author)

Y. Zhang
Institute of Nuclear Energy Safety Technology, Chinese Academy of Sciences
Hefei, Anhui, 230031, China. zymarchine@gmail.com

ABSTRACT

The dynamic foundation-structure interaction (DFSI) problem was formulated in this study by coupling the Isogeometric Analysis (IGA) and the Scaled Boundary Isogeometric Analysis (SBIGA). The unbounded foundation domain was addressed using the SBIGA method, whereas the structural component was formulated using the IGA. These two components were subsequently coupled in the time domain and solved using the Newmark Integration technique.

KEYWORDS

DFSI, IGA, SBIGA, IGA-SBIGA, coupled model.

INTRODUCTION

DFSI problems have been the focus of structural engineers for a long time and various numerical methods have been employed in solving DFSI problems. Among these methods, the finite element massless model and the finite element artificial boundary model have been extensively used, considering the simplicity in their applications. However, the assumptions associated with these two methods introduce inaccuracy to the solution. Zhang et al. (1989) and Zhang et al. (1991) proposed the infinite element method and applied to the dam-foundation interaction analysis. The accuracy of the infinite element method is largely dependent on the radial shape functions. With relatively low-order shape functions, the infinite elements need to be placed far away from the dam body to ensure accuracy. This, however, results in very low computational efficiency.

The Scaled Boundary Finite Element Method (SBFEM) proposed by Song and Wolf (1997) was introduced to solve dam-foundation interaction problems (Yan et al., 2003; Yan et al., 2004). It is used to formulate the acceleration unit-impulse response function, and to derive the interaction force in the form of truncated convolution. This can only improve the computational efficiency to a certain level. Lin et al. (2007) employed SBFEM to address the influence of non-uniform unbounded domain on the response of reservoirs to dynamic impulse. Due to the complications of dam-foundation interaction problems, the number of degrees of freedom on the dam-foundation interface is generally vary large, accordingly the size of the acceleration unit-impulse response matrix.

Isogeometric Analysis (IGA) was proposed by Hughes et al., (2005) to numerically approximate solutions of partial differential equations (PDEs). It is a generalised finite element method (FEM). However, instead of using piecewise polynomials to define basis functions and the computational geometry as in FEM, the computational geometry in IGA is described exactly from the information and the basis functions given by CAD (Computer-Aided Design), and maintained throughout the analysis. IGA has demonstrated to be superior to FEM in terms of handling CAD geometries, convergence on a per-degree-of-freedom basis, and dealing with higher-order differential operators. Combining the concept of SBFEM and IGA, Lin et al. (2014) established a novel numerical framework SBIGA. It inherits the nature of SBFEM by only discretising domain boundaries. However, instead of using low-order Lagrangian polynomials for interpolation, SBIGA employs non-uniform rational B-spline (NURBS) as the basis function to construct and maintain exact geometric models even with coarse meshes. This significantly improves computational efficiency and accuracy.

Based on above-mentioned achievements, this study presented herein aims at developing a coupled IGA-SBIGA scheme to overcome the computational accuracy and efficiency issues when solving DFSI problems. The SBIGA is used to model the unbounded domain, and subsequently coupled with IGA for a highly efficient solution procedure. Under the same grid size, the number of degrees of freedom has been reduced dramatically and hence the size of the acceleration unit-impulse response matrix. This is to provide a more efficient method to solve DFSI problems.

PROBLEM DESCRIPTION

A typical DFSI problem involves three components: the structure, the near-field foundation and the far-field foundation. Normally, the structure and the near-field foundation are considered the generalised structure. Hence, the so-called DFSI problem is actually referring to the interaction between the far-field foundation and the generalised structure separated by the interface, as illustrated in Figure **1**.

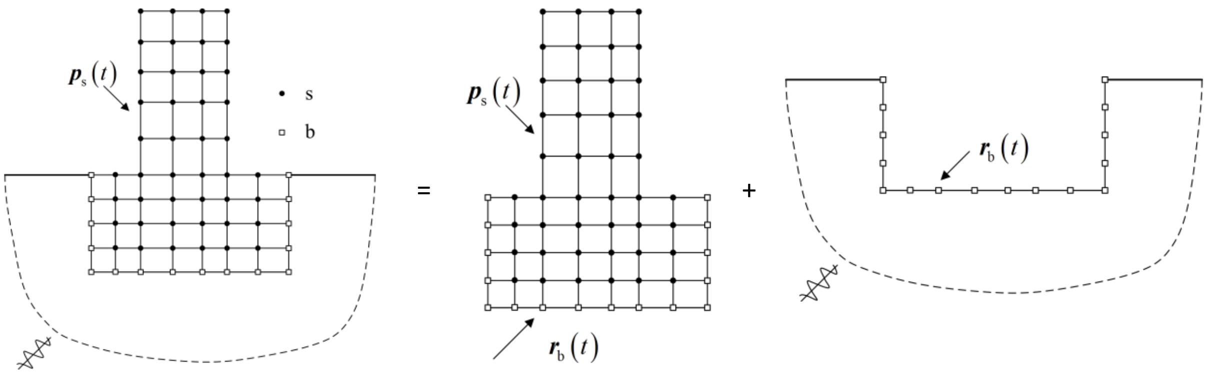

Figure 1. A sketch of the DFSI problem

SBIGA FORMULATION OF UNBOUNDED DOMAIN

Governing Equation

Details of fundamental scaled boundary concept used for formulating the unbounded domain can be referred to in Lin et al. (2014). Here presented is the resulting scaled boundary isogeometric equation in terms of the acceleration unit-impulse response function $\boldsymbol{m}^\infty(t)$ in the time domain:

$$\begin{aligned}&\int_0^t \boldsymbol{m}^\infty(t-\tau)\boldsymbol{m}^\infty(\tau)\mathrm{d}\tau + \boldsymbol{e}^1\int_0^t\int_0^\tau \boldsymbol{m}^\infty(\tau')\mathrm{d}\tau'\mathrm{d}\tau + \int_0^t\int_0^\tau \boldsymbol{m}^\infty(\tau')\mathrm{d}\tau'\mathrm{d}\tau\left(\boldsymbol{e}^1\right)^{\mathrm{T}} \\ &+ t\int_0^t \boldsymbol{m}^\infty(\tau)\mathrm{d}\tau - \boldsymbol{e}^2 t^3 H(t)/6 - \boldsymbol{m}^0 t H(t) = 0\end{aligned} \qquad (1)$$

in which e^1, e^2 and m^0 are SBIGA matrices formulated on domain boundaries and are indepent of time.

Solving $\boldsymbol{m}^\infty(t)$

Eq. (1) is to be discretized to solve $\boldsymbol{m}^\infty(t)$ at discretized time instances $\left[t_0', t_1', t_2', \cdots, t_M'\right]$ with a time step of $\Delta t'$. For any extended interval $\left[t_{m-1}', \bar{t}_m'\right]$ ($\bar{t}_m' = t_{m-1}' + \theta\Delta t'$), $\boldsymbol{m}^\infty(t)$ is assumed linear (see Figure 2). Here, $\theta \in [1,2]$ and is termed the extension factor.

$$\boldsymbol{m}_m^\infty = (\theta-1)\theta^{-1}\boldsymbol{m}_{m-1}^\infty + \theta^{-1}\bar{\boldsymbol{m}}_m^\infty \tag{2}$$

$\boldsymbol{m}_{m-1}^\infty$, $\boldsymbol{m}_m^\infty$ and $\bar{\boldsymbol{m}}_m^\infty$ represent the acceleration unit-impulse response matrix at $t_{m-1}^{'}$, $t_m^{'}$ and $\bar{t}_m^{'}$, respectively.

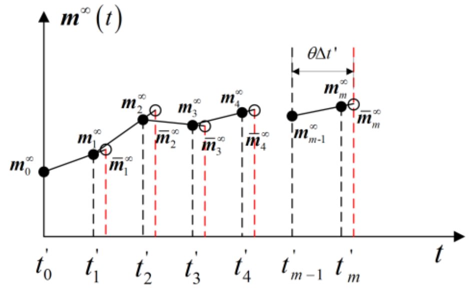

Figure 2. Time discretization of acceleration unit-impulse response matrix

The initial value $\boldsymbol{m}_0^\infty$ can be obtained via:

$$\boldsymbol{M}_0^\infty = \boldsymbol{M}^\infty(t=0) = \boldsymbol{C}_\infty \tag{3}$$

$$\boldsymbol{m}_0^\infty = \left(\boldsymbol{U}^{-1}\right)^{\mathrm{T}} \boldsymbol{C}_\infty \boldsymbol{U}^{-1},\ \boldsymbol{U}^T\boldsymbol{U} = E^0 \tag{4}$$

with C_∞ being the damping matrix when $\omega = 0$.
Introducing the following expressions:

$$\begin{cases} \boldsymbol{I}_0 = 0 \\ \boldsymbol{I}_m = \boldsymbol{I}_{m-1} + 0.5\Delta t^{'}\left(\boldsymbol{m}_{j-1}^\infty + \boldsymbol{m}_j^\infty\right), m \ge 1 \end{cases} \tag{5}$$

$$\begin{cases} \boldsymbol{J}_0 = 0 \\ \boldsymbol{J}_m = \boldsymbol{J}_{m-1} + \Delta t^{'}\boldsymbol{I}_{m-1} + \dfrac{1}{6}\Delta t^{'2}\left(2\boldsymbol{m}_{m-1}^\infty + \boldsymbol{m}_m^\infty\right), m \ge 1 \end{cases} \tag{6}$$

$$I_3\left(t=\bar{t}_1^{'}\right) = \frac{\theta\Delta t^{'}}{6}\left(\bar{\boldsymbol{m}}_1^\infty\right)^2 + \frac{\theta\Delta t^{'}}{3}\boldsymbol{m}_0^\infty\bar{\boldsymbol{m}}_1^\infty + \frac{\theta\Delta t^{'}}{3}\bar{\boldsymbol{m}}_1^\infty\boldsymbol{m}_0^\infty + \frac{\theta\Delta t^{'}}{6}\left(\boldsymbol{m}_0^\infty\right)^2 \tag{7}$$

$$\begin{aligned} I_3\left(t=\bar{t}_2^{'}\right) &= \frac{\Delta t^{'}}{6\theta^2}(\theta-1)^3\left(\bar{\boldsymbol{m}}_2^\infty\right)^2 + \frac{\Delta t^{'}}{6\theta^2}\left(-1+\theta+3\theta^2+\theta^3\right)\left(\boldsymbol{m}_1^\infty\right)^2 \\ &+ \frac{\Delta t^{'}}{6\theta^2}\left(1-2\theta+2\theta^3\right)\left(\boldsymbol{m}_1^\infty\bar{\boldsymbol{m}}_2^\infty + \bar{\boldsymbol{m}}_2^\infty\boldsymbol{m}_1^\infty\right) + \frac{\Delta t^{'}}{6\theta^2}\left(3\theta^2-\theta\right)\left(\boldsymbol{m}_0^\infty\bar{\boldsymbol{m}}_2^\infty + \bar{\boldsymbol{m}}_2^\infty\boldsymbol{m}_0^\infty\right) \\ &+ \frac{\Delta t^{'}}{6\theta^2}\theta\left(\boldsymbol{m}_1^\infty\boldsymbol{m}_0^\infty + \boldsymbol{m}_0^\infty\boldsymbol{m}_1^\infty\right) \end{aligned} \tag{8}$$

$$I_3\left(\bar{t}_m^{'}\right) = \frac{1}{6}\Delta t^{'}\sum_{j=3}^{m-1} conv_j + \boldsymbol{I}_{3r}, m \ge 3 \tag{9}$$

$\boldsymbol{m}^\infty(t)$ can be expressed as:

$$\boldsymbol{m}^\infty(t) = \begin{cases} \boldsymbol{m}_{j-1}^\infty + \dfrac{t-t_{j-1}^{'}}{\Delta t^{'}}\left(\boldsymbol{m}_j^\infty - \boldsymbol{m}_{j-1}^\infty\right), t \in \left[t_{j-1}^{'}, t_j^{'}\right], j = 1,2,\cdots,m-1 \\ \boldsymbol{m}_{m-1}^\infty + \dfrac{t-t_{m-1}^{'}}{\theta\Delta t^{'}}\left(\bar{\boldsymbol{m}}_m^\infty - \boldsymbol{m}_{m-1}^\infty\right), t \in \left[t_{m-1}^{'}, \bar{t}_m^{'}\right] \end{cases}$$

Interaction Force

The nodal force-nodal acceleration relationship in the time domain can be expressed as:

$$\boldsymbol{r}_{b,n} = \boldsymbol{r}_b(t_n) = \int_0^{n\Delta t} \boldsymbol{M}^\infty(\tau)\ddot{\boldsymbol{u}}(n\Delta t - \tau)d\tau = \boldsymbol{r}_{b,n}^{cur} + \boldsymbol{r}_{b,n}^{ini} + \boldsymbol{r}_{b,n}^{his} \tag{10}$$

Here, $\boldsymbol{r}_{b,n}^{cur}$ is associated with the current time step; $\boldsymbol{r}_{b,n}^{ini}$, $\boldsymbol{r}_{b,n}^{his}$ are related to the initial and previous time steps, respectively, and they are written as follows:

$$\boldsymbol{r}_{b,n}^{cur} = \boldsymbol{K}_{bb}^{g}\boldsymbol{u}_n \tag{11}$$

$$\boldsymbol{r}_{b,n}^{ini} = \begin{cases} \boldsymbol{M}_{M-1}^{\infty}\left(K/N\dot{\boldsymbol{u}}_0 - a_{10}\left(\boldsymbol{u}_{n-MN} - \boldsymbol{u}_0\right)\right) \\ \quad + \boldsymbol{M}_{M}^{\infty}\left(\dot{\boldsymbol{u}}_{n-MN} - \left(1+K/N\right)\dot{\boldsymbol{u}}_0 + a_{10}\left(\boldsymbol{u}_{n-MN} - \boldsymbol{u}_0\right)\right) & m = M \\ \boldsymbol{M}_{m}^{\infty}\left(\dot{\boldsymbol{u}}_{n-mN} - \left(1-K/N\right)\dot{\boldsymbol{u}}_0 - a_{10}\left(\boldsymbol{u}_{n-mN} - \boldsymbol{u}_0\right)\right) \\ \quad + \boldsymbol{M}_{m+1}^{\infty}\left(-K/N\dot{\boldsymbol{u}}_0 + a_{10}\left(\boldsymbol{u}_{n-mN} - \boldsymbol{u}_0\right)\right) & 0 < m < M \\ \boldsymbol{M}_{M-1}^{\infty}\left(K/N\dot{\boldsymbol{u}}_0 - a_{10}\left(\boldsymbol{u}_{n-MN} - \boldsymbol{u}_0\right)\right) \\ \quad + \boldsymbol{M}_{M}^{\infty}\left(\dot{\boldsymbol{u}}_{n-MN} - \left(1+K/N\right)\dot{\boldsymbol{u}}_0 + a_{10}\left(\boldsymbol{u}_{n-MN} - \boldsymbol{u}_0\right)\right) & m = M \end{cases} \tag{12}$$

$$\boldsymbol{r}_{b,n}^{his} = \begin{cases} 0 & m = 0 \\ \sum_{i=2}^{m}\boldsymbol{M}_{i}^{\infty}\left(a_{10}\left(\boldsymbol{u}_{n-(i-1)N} - \boldsymbol{u}_{n-iN}\right) - \dot{\boldsymbol{u}}_{n-iN}\right) \\ \quad - \sum_{i=2}^{m}\boldsymbol{M}_{i-1}^{\infty}\left(a_{10}\left(\boldsymbol{u}_{n-(i-1)N} - \boldsymbol{u}_{n-iN}\right) - \dot{\boldsymbol{u}}_{n-(i-1)N}\right) & m > 0 \\ \quad + \boldsymbol{M}_{0}^{\infty}\left(a_{10}\boldsymbol{u}_{n-N} + \dot{\bar{\boldsymbol{u}}}_n\right) - \boldsymbol{M}_{1}^{\infty}\left(a_{10}\boldsymbol{u}_{n-N} + \dot{\boldsymbol{u}}_{n-N}\right) \end{cases} \tag{13}$$

$$\boldsymbol{K}_{bb}^{g} = \left(a_1 - a_{10}\right)\boldsymbol{M}_0^{\infty} + a_{10}\boldsymbol{M}_1^{\infty};\ a_{10} = \frac{1}{N\Delta t} \tag{14}$$

with: $\boldsymbol{K}_{bb}^{g} = \left(a_1 - a_{10}\right)\boldsymbol{M}_0^{\infty} + a_{10}\boldsymbol{M}_1^{\infty};\ a_{10} = \frac{1}{N\Delta t};\ K = n - mN$.

COUPLED IGA-SBIGA FORMULATION OF FSI PROBLEMS

In DFSI problems, the near-field foundation can be described as either a flexible foundation or a rigid foundation. In the former case, the acceleration unit-impulse response matrix is of a size of $N_{dof}^{b} \times N_{dof}^{b}$, with $N_{dof}^{b}{=}s \times N_{cp}^{b}$. N_{dof}^{b} and N_{cp}^{b} are the numbers of degrees of freedom and the controlling points on the interface, respectively. For rigid foundations, the acceleration unit-impulse response function of the unbounded domain will need to be condensed to a 3 by 3 matrix for two-dimensional problems representing translations in two directions and the rotation, or a 6 by 6 matrix for translations in three directions and the associated rotations in three dimensions. In both cases, the coupled IGA-SBIGA solution procedure are the same, apart from condensing the degrees of freedom associated with the structure-foundation interface to those of the rigid foundation.

For the generalised structure, the equations governing structural dynamics, taking into consideration of the influence from unbounded far-field, is written as Eqs. (15) – (21), using a superscript *s* to denote quantities associated the structure:

$$\boldsymbol{M}^{s}\ddot{\boldsymbol{u}}(t_n) + \boldsymbol{C}^{s}\dot{\boldsymbol{u}}(t_n) + \boldsymbol{K}^{s}\boldsymbol{u}(t_n) = \boldsymbol{p}(t_n) \tag{15}$$

$$\boldsymbol{M}^{s} = \begin{bmatrix} \boldsymbol{M}_{ss}^{s} & \boldsymbol{M}_{sb}^{s} \\ \boldsymbol{M}_{bs}^{s} & \boldsymbol{M}_{bb}^{s} \end{bmatrix} \quad \boldsymbol{C}^{s} = \begin{bmatrix} \boldsymbol{C}_{ss}^{s} & \boldsymbol{C}_{sb}^{s} \\ \boldsymbol{C}_{bs}^{s} & \boldsymbol{C}_{bb}^{s} \end{bmatrix} \quad \boldsymbol{K}^{s} = \begin{bmatrix} \boldsymbol{K}_{ss}^{s} & \boldsymbol{K}_{sb}^{s} \\ \boldsymbol{K}_{bs}^{s} & \boldsymbol{K}_{bb}^{s} \end{bmatrix} \tag{16}$$

$$\ddot{\boldsymbol{u}}(t_n) = \begin{Bmatrix} \ddot{\boldsymbol{u}}_s(t_n) \\ \ddot{\boldsymbol{u}}_b(t_n) \end{Bmatrix} \quad \dot{\boldsymbol{u}}(t_n) = \begin{Bmatrix} \dot{\boldsymbol{u}}_s(t_n) \\ \dot{\boldsymbol{u}}_b(t_n) \end{Bmatrix} \quad \boldsymbol{u}(t_n) = \begin{Bmatrix} \boldsymbol{u}_s(t_n) \\ \boldsymbol{u}_b(t_n) \end{Bmatrix} \quad \boldsymbol{p}(t_n) = \begin{Bmatrix} \boldsymbol{p}_s(t_n) \\ -\boldsymbol{r}_b(t_n) \end{Bmatrix} \tag{17}$$

The subscripts *b* and *s* represent qualities associated with the structure and the structure-foundation interface. $\boldsymbol{p}_s(t_n)$ is the time-variant force acting on the structure. $\boldsymbol{r}_b(t_n)$ is the force acting along the structure-foundation interface. Substituting Eq. (10) to Eqs. (15) – (21) results in Eqs. (18) - (20). $\boldsymbol{M}^{s}$ keeps the same format as that in Eq. (15), whereas $\bar{\boldsymbol{K}}^{s}$ is different from $\boldsymbol{K}^{s}$ by modifying the components corresponding to the degrees of freedom of the structure. $\boldsymbol{K}^{s}$, $\boldsymbol{M}^{s}$ and $\boldsymbol{C}^{s}$ are from IGA,

$\boldsymbol{K}_{bb}^{g}$ and $\bar{\boldsymbol{r}}_{b,n}$ are from SBIGA. Eq. (18) is therefore termed the coupled IGA-SBIGA formulation of DFSI problems.

$$\boldsymbol{M}^{\mathrm{s}}\ddot{\boldsymbol{u}}(t_n)+\boldsymbol{C}^{\mathrm{s}}\dot{\boldsymbol{u}}(t_n)+\bar{\boldsymbol{K}}^{\mathrm{s}}\boldsymbol{u}(t_n)=\bar{\boldsymbol{p}}(t_n) \tag{18}$$

$$\bar{\boldsymbol{K}}^{\mathrm{s}}=\begin{bmatrix}\boldsymbol{K}_{\mathrm{ss}}^{\mathrm{s}} & \boldsymbol{K}_{\mathrm{sb}}^{\mathrm{s}}\\ \boldsymbol{K}_{\mathrm{bs}}^{\mathrm{s}} & \bar{\boldsymbol{K}}_{\mathrm{bb}}^{\mathrm{s}}\end{bmatrix} \quad \bar{\boldsymbol{K}}_{\mathrm{bb}}^{\mathrm{s}}=\boldsymbol{K}_{\mathrm{bb}}^{\mathrm{s}}+\boldsymbol{K}_{bb}^{g} \tag{19}$$

$$\bar{\boldsymbol{p}}(t_n)=\begin{Bmatrix}\boldsymbol{p}_{\mathrm{s,n}}\\ -\bar{\boldsymbol{r}}_{\mathrm{b,n}}\end{Bmatrix} \quad \bar{\boldsymbol{r}}_{b,n}=\boldsymbol{r}_{b,n}^{ini}+\boldsymbol{r}_{b,n}^{his} \tag{20}$$

CASE STUDY

A square rigid foundation is embedded in an elastic half-space, with a dimension of b (length) × b (width) × h (depth) (h=2b/3) as shown in Figure 3 (a). An impulse load with a peak value of P_0, described by Figure 3 (b) is applied at the center of the foundation. The elastic half space is featured by a shear modulus of G_s, shear wave velocity of C_s and a possion's ratio of 0.3. Figure 3 (c) shows the SBIGA computational model of the rigid foundation-half space interface, which is discretized into 8 elements in length and width of the foundation, and 4 elements along the depth, resulting in a total of 192 elements.

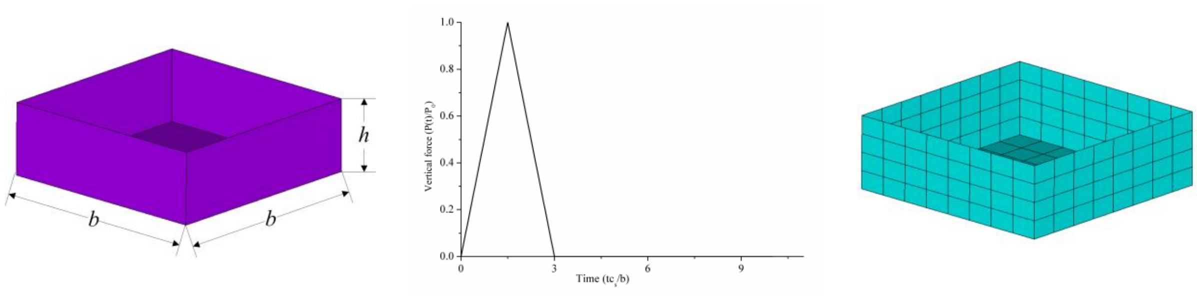

(a) (b) (c)

Figure 3. Sketch of the case study: (a) the rigid foundation; (b) an impulse load and (c)

Adapting the same parameters as used by Radmanović and Katz (2010), the time-vertical displacement relationship is displayed in Figure 4 (a). It can be seen that the results compare well with that in Radmanović and Katz (2010). To examine how the values of θ affects the quality of the numerical calculation, four different θ values were examined: θ = 1.1, 1.2, 1.3 and 1.4, along with three different time intervals of the acceleration unit-impulse response function: $\Delta tc_s/b$ = 0.1, 0.5 and 1, respectively. Results, as displayed in Figure 4 (b), (c) and (d), show that with all chosen $\Delta tc_s/b$ values, the vertical $\boldsymbol{M}^{\infty}(t)$ diverges after a certain time when θ = 1.1. Alternatively, $\boldsymbol{M}^{\infty}(t)$ tends to become more stable when the value of θ increases. It is therefore concluded that θ is a critical factor affecting the quality of the calculation. The greater the θ value, the more stable the calculation. Examining the behaviour of $\boldsymbol{M}^{\infty}(t)$ presented in this case study, it is suggested that a threshold value of θ = 1.4 be used in the calculation procedure.

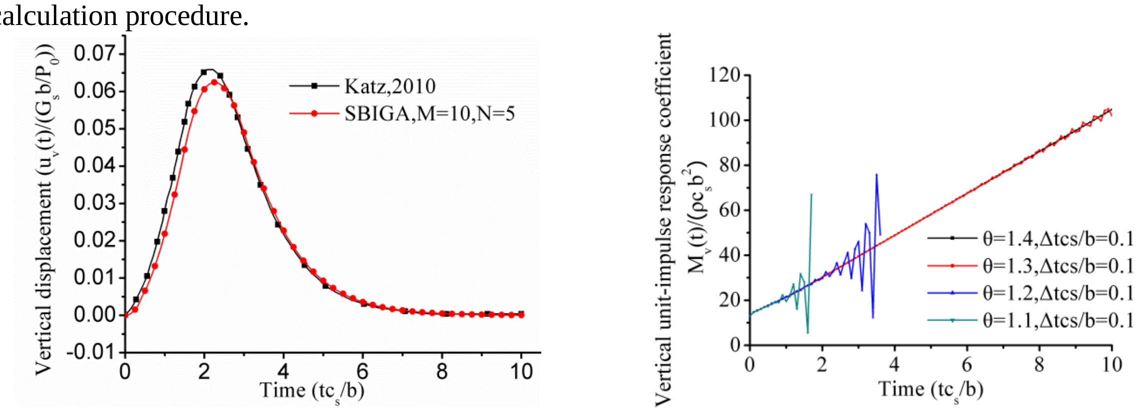

(a) (b)

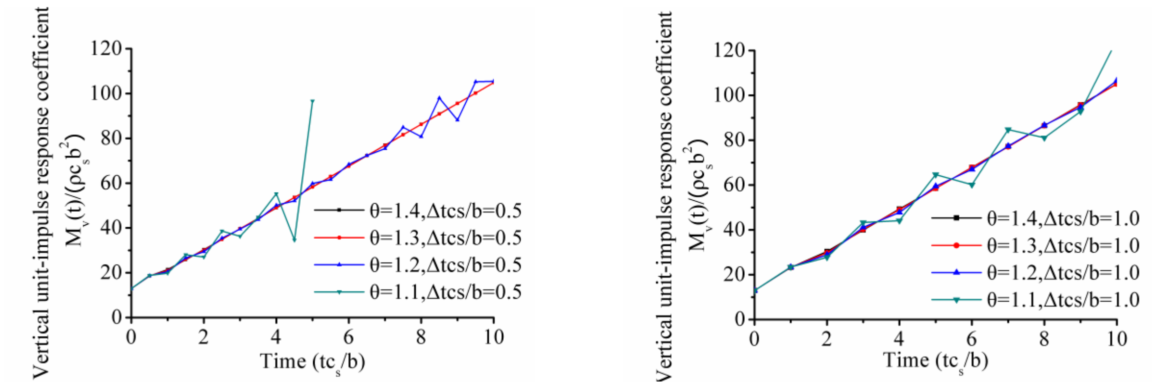

(c) (d)

Figure 4. Results of the case study: (a) comparison of the vertical displacement between Radmanović and Katz (2010) and the present study; (b) vertical $\boldsymbol{M}^{\infty}(t)$ with $\Delta tc_s/b$ = 0.1 with varying θ;(c) vertical $\boldsymbol{M}^{\infty}(t)$ with $\Delta tc_s/b$ = 0.5 and varying θ, and (d) vertical $\boldsymbol{M}^{\infty}(t)$ with $\Delta tc_s/b$ = 1.0 with varying θ.

CONCLUSIONS

A coupled IGA-SBIGA procedure is formulated in this study to address DFSI problems. The influence of the unbounded domain was considered by formulating a SBIGA model on the structure-foundation interface. The structure is modelled by using the IGA. These two components were subsequently coupled to develop an IGA-SBIGA DFSI formulation and solved using the Newmark integral method in the time domain. Parametric analysis in terms of the extension factor θ recommended that a threshold value of 1.4 should be considered to ensure the stability of the calculation. The proposed algorithm can be applied to solve more generalised problems involving both bounded and unbounded domains, such as dam-foundation interaction and wave-structure interaction problems, and makes solving real engineering problems in three dimensions computationally feasible and efficient.

REFERENCES

Lin, G., Du, J., Hu, Z., (2007). Earthquake analysis of arch and gravity dams including the effects of foundation inhomogeneity. *Frontiers of Architecture and Civil Engineering in China* (1), 41-50.

Lin, G., Zhang, Y., Hu, Z., Zhong, H., 2014. Scaled boundary isogeometric analysis for 2D elastostatics. *Science China Physics, Mechanics and Astronomy* 57 (2), 286-300.

Radmanović, B., Katz, C., 2010. A high performance scaled boundary finite element method. *IOP Conference Series: Materials Science and Engineering* 10 (1), 012214.

Song, C., Wolf, J.P., 1997. The scaled boundary finite-element method—alias consistent infinitesimal finite-element cell method—for elastodynamics. *Computer Methods in Applied Mechanics and Engineering* 147 (3–4), 329-355.

Hughes, T.J., Cottrell, J.A., Bazilevs, Y., 2005. Isogeometric analysis: CAD, finite elements, NURBS, exact geometry and mesh refinement. Computer Methods in Applied Mechanics and Engineering 194 (39), 4135-4195.

Yan, J., Jin, F., Xu, Y., Wang, G., Zhang, C., 2003. A seismic free field input model for FE-SBFE coupling in time domain. *Earthquake Engineering and Engineering Vibration* 2 (1), 51-58.

Yan, J., Zhang, C., Jin, F., 2004. A coupling procedure of FE and SBFE for soil–structure interaction in the time domain. *International Journal for Numerical Methods in Engineering* 59 (11), 1453-1471.

Zhang, C., Song, C., Pekau, O.A., 1991. Infinite boundary elements for dynamic problems of 3-D half space. *International Journal for Numerical Methods in Engineering* 31 (3), 447-462.

Zhang, C., Song, C., Wang, G., Jin, F., 1989. 3-D infinite boundary elements and simulation of monolithic dam foundations. *Communications in Applied Numerical Methods* 5 (6), 389-400.